INVESTIGATION OF THE TURBULENT MASS TRANSPORT DURING THE MIXING OF A STABLE STRATIFICATION WITH A FREE JET USING CFD-METHODS

I1. Armin Zirkel, I2. Eckart Laurien

Institute of Nuclear Technology and Energy Systems, Universität Stuttgart

Abstract

During a severe accident, hydrogen can be produced by a chemical reaction between the Zircaloy cladding and water and escape into the containment through a leak in the primary circuit. The prediction of the mass transport of hydrogen is vital for an optimized positioning of countermeasures like recombiners. It is possible that a stable stratification of hydrogen and air occurs, due to the different densities of those fluids. This paper discusses the simulation of mass transport processes during the mixing of such a stable stratification with a free jet. The mixing of a stable stratification with a free jet is characterized by the time dependency of the flow, sharp velocity and density gradients as well as the non-isotropy of Reynolds stresses and turbulent mass fluxes. This paper discusses results of the eddy diffusivity model for the turbulent mass flux as well as improvements with the use of a newly implemented non-isotropic model.

1. INTRODUCTION

This paper presents the current state of an ongoing analysis and validation of turbulence models for computational fluid dynamics (CFD) for containment flows after a loss-of-coolant accident (LOCA) in an existing light water reactor. The topic of this work is to investigate turbulence modeling for the mixing of a stable stratification with an intruding turbulent free jet. Both, the free jet and the stable stratification are causing non-isotropic turbulence. Buoyancy turbulence production also has an influence, as turbulence is not only produced by shear stresses.

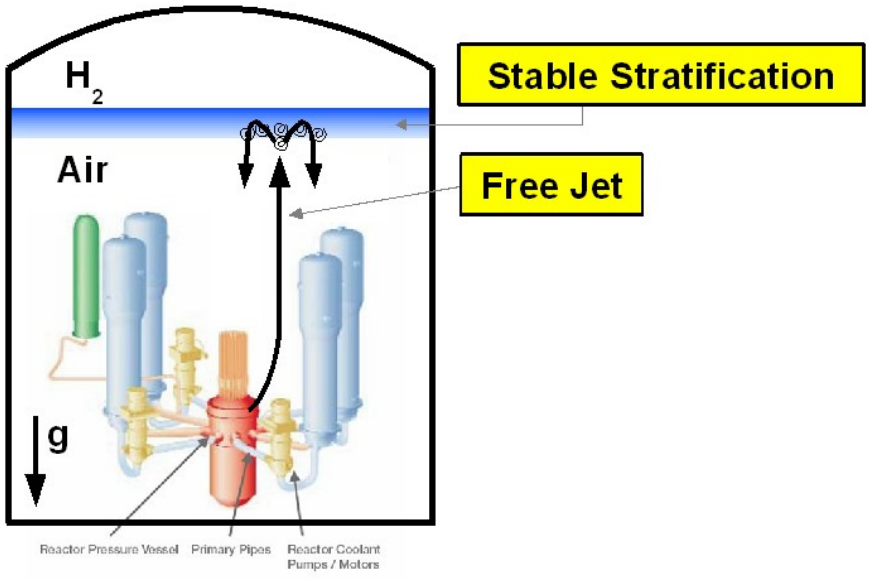

Fig. 1: Stable stratification inside a containment

Lumped parameter models have been developed, verified and used to analyze and predict transport processes within a containment (Fig. 1) (Allelein, 2005; Allelein, 2008). These models are based on mass and energy budgets between given control volumes inside a containment building. They can provide valuable information about complex flows, such as mixing, condensation and aerosol transport. However, flow models are often specialized to a narrow range of application and the user influence is rather large. Recently, methods of computational fluid dynamics have also been used to simulate containment flows (Kljenak, 2006; Houkema, 2008). They are based on temporally averaged mass, momentum and energy conservation equations, which appear as a set of coupled partial differential equations. Their turbulence models, see Laurien (2007) for an overview, can be applied to a wide range of flow situations and geometries, represented by a fine boundary fitted numerical grid. The Reynolds stress turbulence models are capable of yielding good results for flows with non-isotropic turbulent stresses. Models to calculate non-isotropic turbulent fluxes are available (Rodi, 1993) but not implemented in commercial software. Currently, the mixing of a stable stratification calculated by CFD takes longer time than measured mixing due to the isotropic calculation of the turbulent fluxes.

The aim of this work is to develop a formulation of a non-isotropic turbulent flux model that is able to predict the mixing of a stable stratification. This new turbulent flux model can replace the eddy diffusivity concept in the Reynolds stress turbulence models. In order to do this, the influence of buoyancy turbulence production as well as the impact of the isotropic approach of eddy viscosity models is investigated.

To get detailed information about the turbulence, a theoretical steady state test case is designed. A large eddy simulation (LES) is performed to be the reference case.

2. EXPERIMENT

Experiments for containment flows are the THAI-experiments (Thermohydraulic, Hydrogen/Helium, Aerosol and Iodine) performed by Becker Technologies. The experiments referred to in this paper are the TH20 experiments (Kanzleiter, 2007). Fig. 2 shows a model of the geometry and a schematic representation of the experiment.

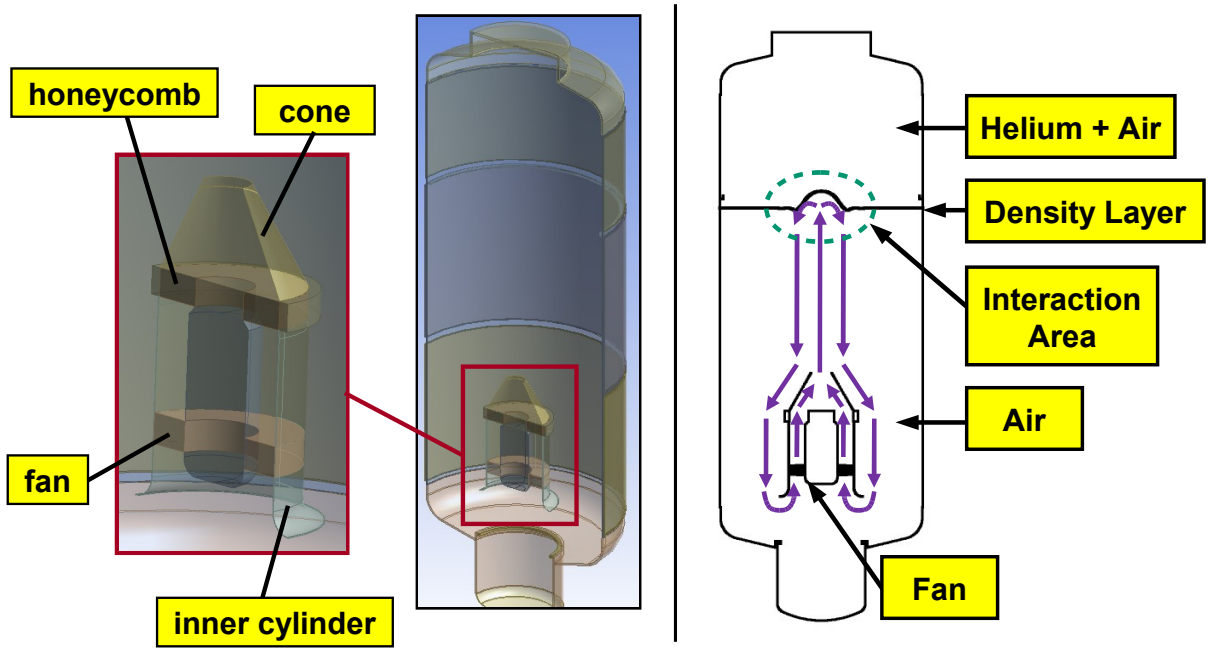

Fig. 2: left: TH20 geometry model; right: TH20 scheme

The height of the vessel is 9.2m with a diameter of 3.16m. The configuration of the THAI-vessel for TH20 contains a short inner cylinder in the lower vessel with a diameter of 1.4m. Inside the inner cylinder is the fan that generates the free jet. For safety reasons, helium is used instead of hydrogen for the TH20 experiments.

Before the actual experiment, the stable stratification is created. Helium is carefully brought into the THAI-vessel to prevent mixing due to the incoming mass flow of helium. This results in a stable stratification, because the less dense fluid accumulates in the upper vessel and is on top of the denser fluid. The sharp density gradient between the light gas cloud on top and air below is denoted as density layer. It is the reason for the non-isotropic turbulence because the gradient only appears normal to the density layer.

After the creation of the stratification is complete, a free jet is generated by the fan inside the inner cylinder of the vessel. The jet tends to penetrate the density layer but is reflected because the layer is stable. During the redirection process, the jet takes in helium and erodes the density layer. The duration of the experiment, from the start of the fan until the helium distribution inside the vessel is homogeneous, is 13 minutes.

3. GOVERNING EQUATIONS

The governing equations for CFD with turbulence models are the Reynolds averaged Navier-Stokes-equations (RANS) with the concentration equation (1) for the mass transport.

$$\frac{\partial(\bar{\rho}\tilde{\varphi})}{\partial t}+\frac{\partial(\bar{\rho}\tilde{u}_i\tilde{\varphi})}{\partial x_i}=\frac{\partial}{\partial x_i}\left(\lambda\frac{\partial\tilde{\varphi}}{\partial x_i}-\widetilde{u_i'\varphi'}\right) \tag{1}$$

The concept of Reynolds averaging is the averaging of the turbulent values over time, which are then determined by an appropriate turbulence model (Rodi, 1993). In commercial CFD code, the turbulent mass fluxes $\widetilde{u_i'\varphi'}$ are calculated with the isotropic eddy diffusivity model (2).

$$-\widetilde{u_i'\varphi'}=\Gamma_t\cdot\frac{\partial\tilde{\varphi}}{\partial x_i} \tag{2}$$

The eddy diffusivity is the eddy viscosity divided by a constant turbulent Schmidt number $\Gamma_t=\frac{\nu_t}{\sigma_t}$. This value is used to determine the turbulent mass flux in every direction. The turbulent scalar flux model (TSF) has a transport equation for each spatial direction (3) and the variance (4). With this four additional equations, the non-isotropy of turbulent mass fluxes can be calculated.

$$\begin{aligned}\frac{\partial}{\partial t}\left(\widetilde{u_i'\varphi'}\right)+\frac{\partial}{\partial x_j}\left(\tilde{u}_j\widetilde{u_i'\varphi'}\right)=&-\widetilde{u_i'u_j'}\frac{\partial\tilde{\varphi}}{\partial x_j}-\widetilde{u_j'\varphi'}\frac{\partial\tilde{u}_i}{\partial x_j}\\&-\left(1-C_{3Y}\right)\beta\frac{\widetilde{\varphi'^2}}{\rho}\left(\frac{\partial\bar{p}_{stat}}{\partial x_i}+\rho_{ref}\,g_i\right)\\&+\frac{\partial}{\partial x_j}\left[\left(\mu+\frac{2}{3}C_Y\frac{\hat{k}^2}{\hat{\epsilon}}\bar{\rho}\right)\frac{\partial}{\partial x_j}\left(\frac{\widetilde{u_i'\varphi'}}{\bar{\rho}}\right)\right]\\&-C_{1Y}\frac{\hat{\epsilon}}{\hat{k}}\widetilde{u_i'\varphi'}-C_{2Y}\widetilde{u_j'\varphi'}\frac{\partial\tilde{u}_i}{\partial x_j}-C_{4Y}\widetilde{u_j'\varphi'}\frac{\partial\tilde{u}_j}{\partial x_i}\end{aligned} \tag{3}$$

$$\frac{\partial}{\partial t}\left(\widetilde{\varphi''^2}\right)+\frac{\partial}{\partial x_j}\left(\tilde{u}_j\widetilde{\varphi''^2}\right)=-2\widetilde{u_j''\varphi''}\frac{\tilde{\varphi}_l}{\partial x_j}+\frac{\partial}{\partial x_j}\left[\left(\mu+\frac{2}{3}C_{YY}\frac{\hat{k}^2}{\hat{\epsilon}}\bar{\rho}\right)\frac{\partial}{\partial x_j}\left(\frac{\widetilde{\varphi''^2}}{\bar{\rho}}\right)\right]-2C_{1YY}\frac{\hat{\epsilon}}{\hat{k}}\widetilde{\varphi''^2} \quad (4)$$

The model contains several coefficients, C_Y, C_{1Y}, C_{2Y}, C_{3Y}, C_{4Y}, C_{YY} and C_{1YY}, which are to be adjusted as part of this work.

4. STEADY STATE TEST CASE

An important factor for turbulence modeling is the comparability of different calculations. For the present case of eroding a stable stratification with a free jet, spatial comparison is necessary because the mixing happens locally. So a transient case is disadvantageous, because the time has always to be considered when comparing spatial distributions of turbulent values. Therefore a theoretical steady state test case is designed (Fig. 3).

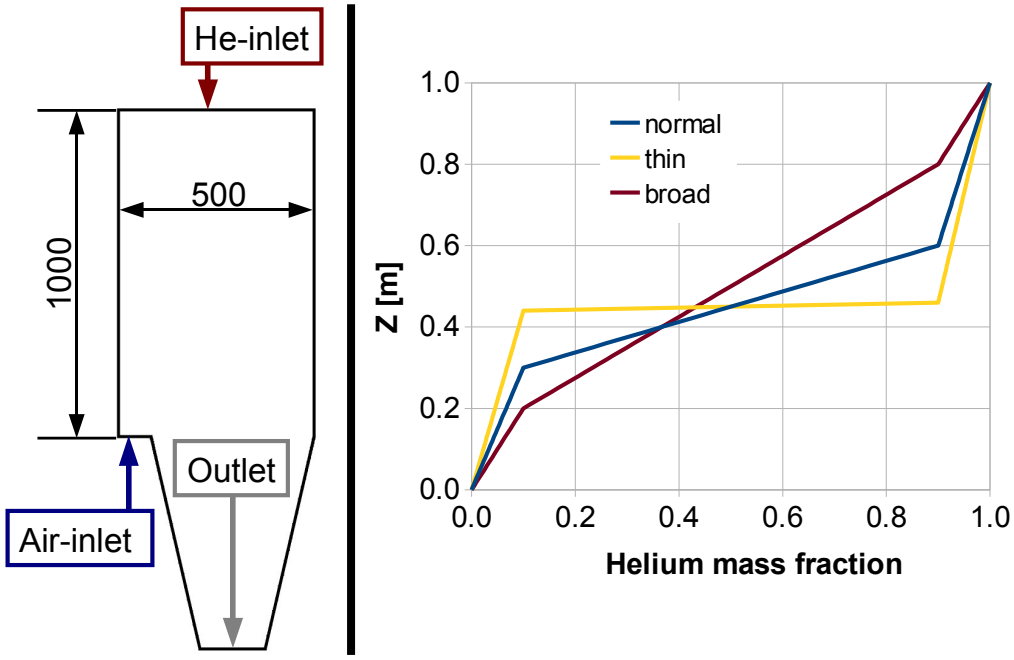

Fig. 3: left: Scheme of the steady state test case; right: initial helium distribution

The geometry is an open cylinder with height h = 1000 mm and radius r = 500 mm. Air is flowing with 2 m/s into the domain through the air-inlet, generating a free jet. To create a steady state, an equal amount of helium that left the domain through the outlet is reinserted through the helium-inlet. The outgoing mass-flow of helium is also a value for the mixing quality of the used turbulence model. A larger helium outflow means a better mixing of the turbulence model.

A stable stratification is given through an initial helium distribution. Fig. 3 shows three different initial distributions, where the mass of helium is 70.42 g for the thin, 78.87 g for the normal and 84.34 g for the broad initial distribution. A preliminary investigation shows no influence of the initial distribution on the shape or thickness of the final stratification. The height of the layer varies with the amount of helium.

5. DIMENSION ANALYSIS

5.1 Dimension Matrix

To ensure that the test case is a reasonable representation of the TH20 case, a dimension analysis is performed to determine independent dimensionless numbers to compare those cases (Szirtes, 2007). A set of seven parameters describes the TH20 case at a given time. Those parameters are the length L of the jet which is the distance between the nozzle and the stable stratification, the velocity u of the jet, the density ρ, the density difference Δρ between the jet and the light-gas cloud, the viscosity ν, the gravity g and the diffusion constant D. The three base units for those parameters are m, s and kg.

Seven parameters with three base units means that there are four independent dimensionless numbers. The expected relevant dimensionless numbers for this dimension analysis are the Reynolds number Re, the Richardson number Ri, the Archimedes number Ar and the Schmidt number Sc. The Reynolds number is the ratio of inertial forces to viscous forces. The Richardson number is the ratio of potential to kinetic energy. The Archimedes number is the ratio of buoyancy forces to friction forces. The Schmidt number is the ration of convective to diffusive mass transport.

Table 1: Paramters for the dimension analysis

L	u	ρ	Δρ	ν	g	D	Re	Ri	Ar	Sc
m	$\frac{m}{s}$	$\frac{kg}{m^3}$	$\frac{kg}{m^3}$	$\frac{m^2}{s}$	$\frac{m}{s^2}$	$\frac{m^2}{s}$	$\frac{L \cdot u}{\nu}$	$\frac{g \cdot L}{u^2}$	$\frac{\Delta\rho \cdot g \cdot L^3}{\rho \cdot \nu^2}$	$\frac{\nu}{D}$

To prove that the dimensional numbers are independent, the determinant of the dimension matrix must not be zero. The dimension matrix (Fig. 4) is the correlation of the describing parameters and the base units and dimensionless numbers.

	L	u	ρ	$\Delta\rho$	ν	g	D
m	1	1	−3	−3	2	1	2
s	0	−1	0	0	−1	−2	−1
kg	0	0	1	1	0	0	0
Re	1	1	0	0	−1	0	0
Ri	1	−2	0	0	0	1	0
Ar	3	0	−1	1	−2	1	0
Sc	0	0	0	0	1	0	−1

Fig. 4: Dimension matrix

Every parameter has its column and every base unit and dimensionless number has its row. The values of the matrix are the exponents with which the base units appear in the dimension of the parameter or the exponent with which the parameter appears in a dimensionless number. For example, velocity has the dimension m/s. So the value for meter is 1 and for second -1. Velocity appears with the exponent 1 in the Reynolds number and with -2 in the Richardson number. The determinant of the dimension matrix is -56, so it is demonstrated, that the dimensionless parameters are independent.

5.2 Parameters

The length of the free jet, which is the distance between the nozzle outlet and the stable stratification, is the characteristic length.

$$L_{test} = 0.66\,m;\; L_{TH20} = 2.27\,m$$

The maximum velocity of the free jet is taken as the characteristic velocity.

$$u_{test} = 2.013\frac{m}{s};\; u_{TH20} = 1.827\frac{m}{s}$$

Reference density is the density of air, $\rho_{Air} = 1.185\frac{kg}{m^3}$. For the density differences, the density of the light gas cloud is necessary. In the test case, the light gas cloud is pure helium with a density of $\rho_{He} = 0.1785\frac{kg}{m^3}$. In the TH20 case, the cloud has 36% helium and a density of $\rho_{He} = 0.84\frac{kg}{m^3}$

The characteristic density difference is the difference between air and the light gas cloud.

$$\Delta\rho_{test} = \rho_{Air} - \rho_{He} = 1.0065\frac{kg}{m^3};\; \Delta\rho_{TH20} = \rho_{Air} - \rho_{Mix} = 0.345\frac{kg}{m^3}$$

The kinematic viscosity is

$$\nu_{test} = \frac{1}{2}\left(\nu_{Air} + \nu_{He}\right) = \frac{1}{2}\left(1.545\cdot10^{-5}\frac{m^2}{s} + 10.4202\cdot10^{-5}\frac{m^2}{s}\right) = 5.9826\cdot10^{-5}\frac{m^2}{s}$$

$$\nu_{TH20} = \frac{1}{2}\left(\nu_{Air} + \nu_{Mix}\right) = \frac{1}{2}\left(1.545\cdot10^{-5}\frac{m^2}{s} + 2.183\cdot10^{-5}\frac{m^2}{s}\right) = 1.864\cdot10^{-5}\frac{m^2}{s}$$

The gravity constant is $g = 9.81\frac{m}{s^2}$ and the diffusion constant for helium and air $D = 26.5\frac{cm^2}{s}$.

5.3 Dimensionless numbers

Table 2 shows the dimensionless numbers for both cases. The Reynolds number indicates a fully turbulent flow for both cases. The Richardson number shows a slight dominance of the potential energy in both cases.. The Archimedes number in both cases is very large. This stands for a domination of the buoyancy forces. The Schmidt number is almost the same for both cases. It is possible to have an even better match of both cases, but this would lead to a larger computational domain which increases the computational effort.

Table 2: Dimensionless numbers

	Re	Ri	Ar	Sc
Test case	$2.22\cdot10^4$	1.6	$6.69\cdot10^8$	0.02
TH20	$2.22\cdot10^5$	6.67	$7.8\cdot10^{10}$	0.01

6. IMPACT OF THE EDDY DIFFUSIVITY MODEL

All two-dimensional simulations are carried out on a two-dimensional equidistant structured grid which meets all criteria of the best practice guideline for CFD code validation for reactor-safety applications (Menter, 2002). A grid dependency study shows no grid influence on the result.

To investigate the impact of the turbulence model, two simulations are performed, one with a eddy viscosity model (kω) and on with a Reynolds stress model (ωRSM). Both simulations use the eddy

diffusivity model to calculate the turbulent mass fluxes. The simulations are carried out

The helium outflow of the simulation using the kω-model is $He_{out}=3.31\frac{g}{s}$. With the ωRSM $He_{out}=3.37\frac{g}{s}$. Fig. 5 gives a comparison of the results for the helium mass fraction and the vertical velocity. Both distributions are almost identical for both turbulence models.

This shows that the result is dominated by the model for the mass flux and the impact of the turbulence model is negligible.

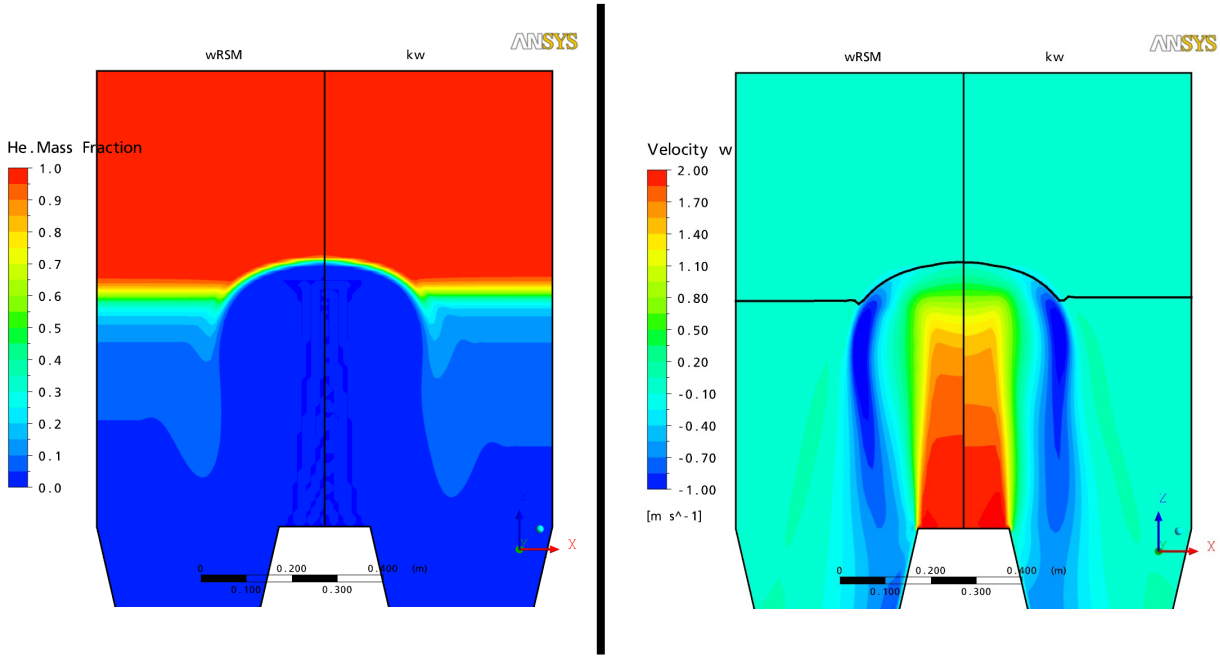

Fig. 5: Comparison ωRSM ↔ kω, left: helium mass fraction; right: vertical velocity

7. Large Eddy Simulation

A Large Eddy Simulation directly simulates the large, energy bearing eddies. A subgrid-scale model is used for the eddies that are too small to be resolved by the grid. Therefore a LES has high demands on the quality of the grid. To get meaningful results, the inertial range of Kolmogorov's energy cascade has to be resolved (Fröhlich, 2007).

The left hand side of Fig. 6 shows a generic turbulent spectrum (energy E over wave-number k). The three important regions are the large eddies with lower wave-numbers, the inertial range and the dissipation range with high wave-numbers. The typical slope of the inertial range is $k^{-\frac{5}{3}}$.

To check the quality of the LES, turbulent spectra must be analyzed as part of the post-processing. The right hand side of Fig. 6 shows a representative turbulent spectrum of the performed LES for the steady state test case. It shows that the inertial range with its characteristic slope is resolved by the grid. Therefore it can be assumed, that the grid quality is sufficient. To verify this assumption, a second LES with a considerably finer grid will be performed to investigate a possible impact of a simulation of smaller eddies on the result.

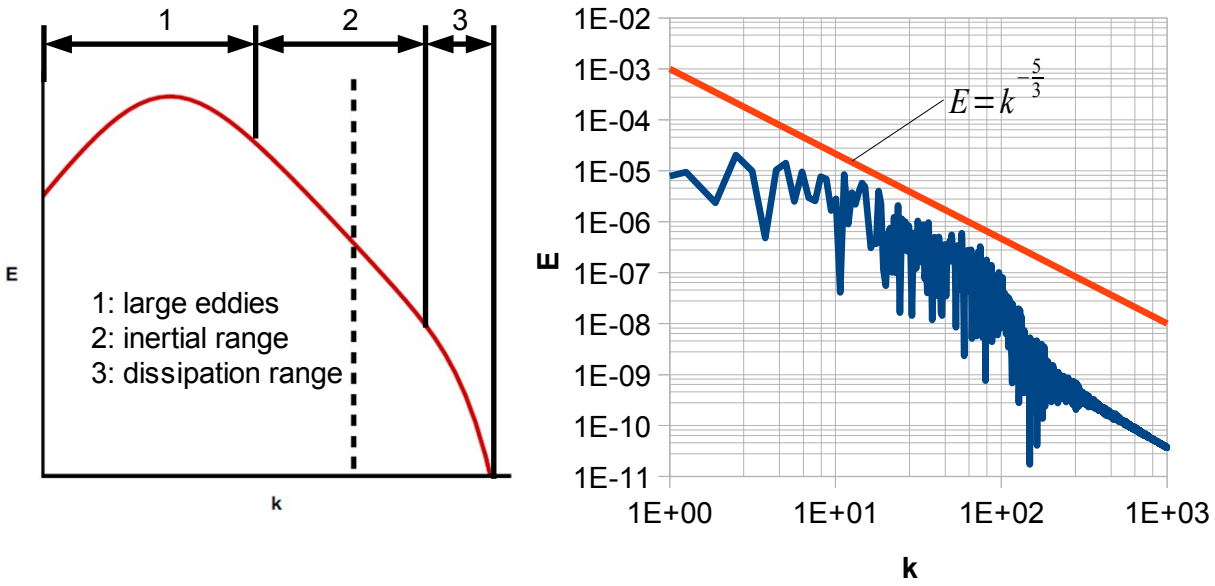

Fig. 6: Turbulent spectrum

The grid used for this LES is a three-dimensional block-structured grid with $2.5 \cdot 10^6$ nodes. The central differences advection scheme is used. The time step is 0.001 s with the 2nd order backward Euler transient scheme. Small eddies are modeled with the Smagorinski subgrid-scale model. The simulation is carried out on 64 CPUs. It takes 24 hours to simulate 0.8 s physical time.

After 10 seconds physical time, a statistically steady state is reached. The transient averaged results are averaged over additional 10 seconds physical time. The helium outflow is $He_{out,\,LES} = 3.8 \frac{g}{s}$, which is $0.49 \frac{g}{s}$ more than with the eddy diffusivity and kω-model.

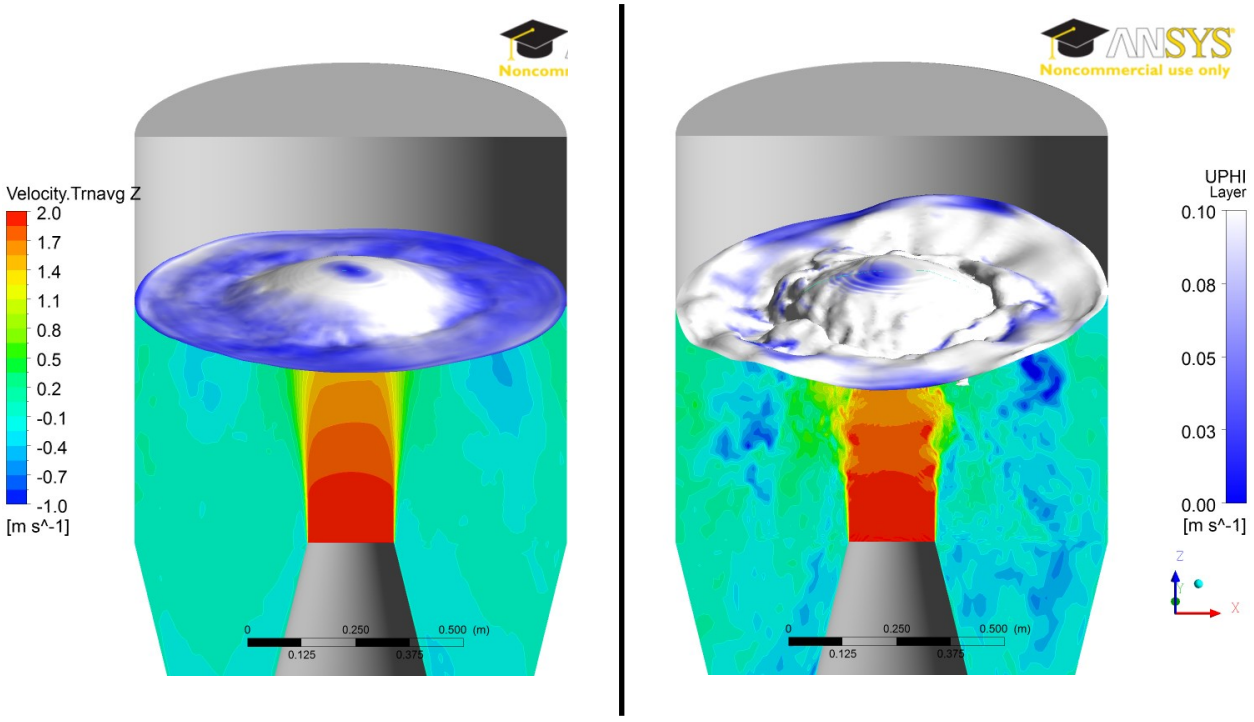

Fig. 7: Vertical velocity, density layer and mass flux; left: transient averaged; right: instantaneous

Fig. 7 shows the helium layer, which is defined as an isosurface of 50% helium. It is colored with the turbulent mass flux of helium $\widetilde{u'\varphi'}$. The xz-plane below the layer shows the vertical velocity. A comparison of the averaged (Fig. 7, left) and instantaneous (Fig. 7, right) helium layer shows strong three-dimensional, transient effects, despite the symmetric geometry and boundary conditions. The interaction between the jet and the stable stratification causes the jet to move unpredictable around the symmetry axis of the geometry without a preferred direction. However, transient averaging shows that the result is symmetric.

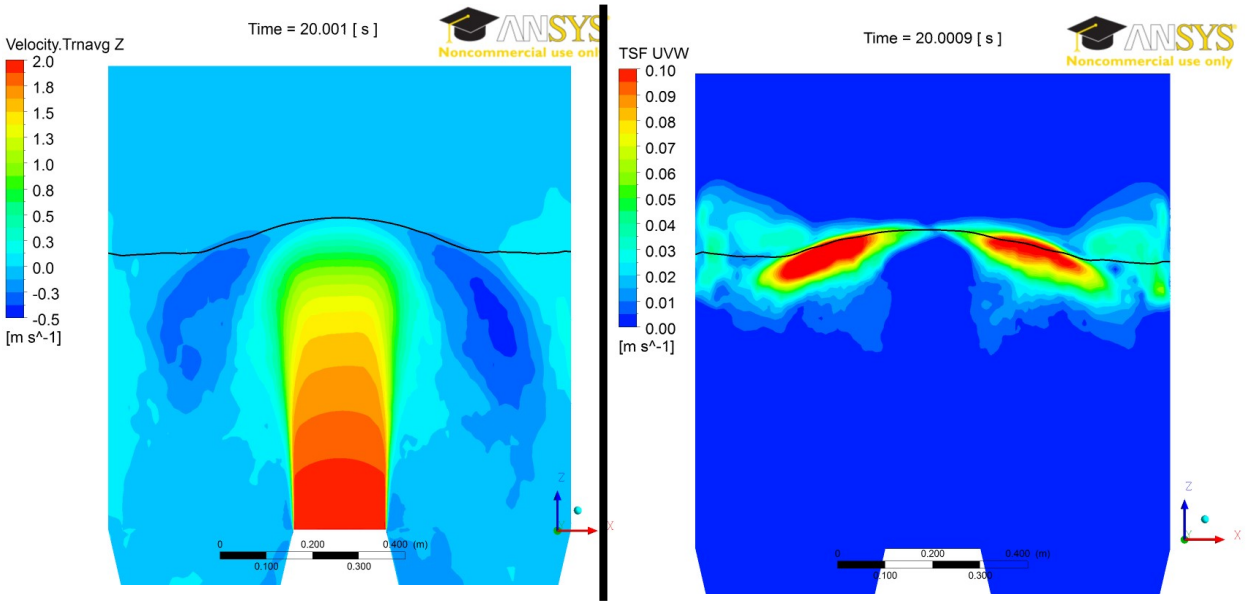

Fig. 8: Transient averaged values; left: Vertical velocity; right: Turbulent mass flux

The left hand side of Fig. 8 shows the transient averaged vertical velocity of the LES. As opposed to the free jet calculated with the eddy diffusivity model (Fig. 5), the down-flow region of the jet is less distinct. It is broader and reaches to the wall of the vessel. The maximum velocity of the down-flow is $0.5\frac{m}{s}$ where simulations with the eddy diffusivity model yield a faster down-flow with $1\frac{m}{s}$. This is an effect of the three-dimensional movement of the flow in the LES case, which can not be captured in the two-dimensional RANS simulations.

Fig. 7 (left) and Fig. 8 (right) show, that the primary turbulent mass flux is in the redirection region of the free jet. The possible impact of the three-dimensional movement of jet and layer on the mixing is not yet determined.

8. CONCLUSION

Simulations of the TH20 experiment has shown that currently available commercial cfd-software has no turbulence model to predict the mixing of a stable stratification with a free jet. To improve this situation, the Turbulent Scalar Flux model will be tested and adjusted for this case. To accomplish this, a theoretical steady state test case was designed to improve the comparability of different simulations. This also provides a more detailed view on specific physical aspects like the turbulent mass fluxes.

A dimension analysis has shown, that the test case is a reasonable representation of the TH20 experiment. The defining dimensionless numbers are the Reynolds, Richardson, Archimedes and Schmidt number.

Preliminary, two-dimensional simulations were performed to investigate the impact of the turbulence model compared to the model for the turbulent mass fluxes. An eddy viscosity model (kω) and a Reynolds stress model (ωRSM) were used for this investigation. Both simulations were using the eddy diffusivity model to calculate the turbulent mass fluxes. It turned out, that the eddy diffusivity model dominates the result.

A large eddy simulation was performed as the reference case. The used grid has $2.5 \cdot 10^6$ nodes, which is sufficient to resolve the inertial range of the energy cascade. The geometry as well as the boundary conditions are symmetric, but the interaction of the free jet and the stable stratification causes an unpredictable three-dimensional, transient behavior of the flow. The transient averaged result is symmetric. The calculated helium outflow is up to $0.49 \frac{g}{s}$ larger than the outflow of the preliminary simulations which indicates that the helium mixing is better in the LES case.

Another difference between the preliminary RANS simulations and the LES is the down-flow between helium layer and outlet boundary.

A second LES on a finer grid will be performed to investigate a possible impact of the resolution of smaller eddies on the result.

For a more detailed investigation of the three-dimensional behavior, two- and three-dimensional RANS-simulations will be carried out. The eddy diffusivity model and the new turbulent scalar flux model will be used. As part of this investigation, the model coefficients of the turbulent scalar flux model will be adjusted. The adjusted model will then be used to calculate the original TH20 experiment.

ACKNOWLEDGMENTS

This work has been supported by the German Bundesministerium für Wirtschaft und Technologie (BMWi), GRS 1501339

REFERENCES

H.-J. Allelein, S. Arndt, W. Klein-Heßling, S. Schwarz, C. Spengler, G. Weber: "COCOSYS: Status of development and validation of the German containment code system", Nuclear Engineering and Design, 238, 872-889 (2008)

H.-J. Allelein, K. Neu, J.P. Van Dorsselaere: "European validation of the Integral Code ASTEC (EVITA) – first experience in validation and sequence calculation", *Nuclear Engineering and Design*, 235, 285-296 (2005)

I. Kljenak, M. Mabic and I. Bajsic: "Modeling of Containment Atmosphere Mixing and Stratification Experiment using a CFD Approach", *Nuclear Engineering and Design*, 236, 1683-1692 (2006)

M. Houkema, N.B. Siccama, J. A. Lycklama à Nijeholt, E. M. J. Komen: "Validation of the CFX4 CFD code for containment thermal-hydraulics", *Nuclear Engineering and Design*, 238, 590-599 (2008)

E. Laurien: "Turbulence Modeling for CFD in Reactor Safety", *Proc. Ann. Meeting on Nuclear Techology*, Karlsruhe, May 22-24, 2007, Inforum GmbH, Bonn

W. Rodi: *Turbulence Models and Their Applications in Hydraulics*, A. A. Balkema (1993)
T. Kanzleiter, A. Kühnel. K. Fischer, M. Heitsch, B. Schramm: "THAI Blower Test TH20", *GRS Reactor Safety Research*, Report No. 150 1325 - TH20 (2007)
T. Szirtes: *Applied Dimensional Analysis and Modeling*, Elsevier (2007)
F. Menter: CFD Best Practice Guidelines for CFD Code Validation for Reactor-Safety Applications, EVOL-ECORA-D01 (2002)
J. Fröhlich: *Large Eddy Simulation turbulenter Strömungen*, Teubner (2006)